Available online at www.sciencedirect.com
SCIENCE DIRECT
European Journal of Pharmaceutics and Biopharmaceutics 60 (2005) 81–89
European Journal of Pharmaceutics and Biopharmaceutics
www.elsevier.com/locate/ejpb

Research paper

Comparison of powder produced by evaporative precipitation into aqueous solution (EPAS) and spray freezing into liquid (SFL) technologies using novel Z-contrast STEM and complimentary techniques

Jason M. Vaughn[a], Xiaoxia Gao[b], Miguel-Jose Yacaman[b], Keith P. Johnston[b,1], Robert O. Williams III[a,*]

[a]College of Pharmacy, University of Texas at Austin, Austin, TX, USA
[b]Department of Chemical Engineering, University of Texas at Austin, Austin, TX, USA

Received 3 October 2004; accepted in revised form 10 January 2005
Available online 23 March 2005

Abstract

The objective of this study was to compare the properties of particles formed by nucleation and polymer stabilization (e.g. evaporative precipitation into aqueous solution (EPAS)) versus rapid freezing (e.g. spray freezing into liquid (SFL)). Powders formed by EPAS and SFL, composed of danazol and PVP K-15 in a 1:1 ratio, were characterized using X-ray powder diffraction, modulated differential scanning calorimetry (MDSC), contact angle determination, dissolution, scanning electron microscopy (SEM), environmental scanning electron microscopy (ESEM), BET specific surface area, and Z-contrast scanning transmission electron microscopy (STEM). Large differences in particle morphologies and properties were observed and explained in terms of the particle formation mechanisms. Both techniques produced amorphous powders with high T_g and low contact angle values. However, STEM analysis showed highly porous bicontinuous nanostructured 30 nm particles connected by narrow bridges for SFL versus aggregated 500 nm primary particles for EPAS. The combination of STEM and other characterization techniques indicates solid solutions were formed for the SFL powders consistent with rapid freezing. In contrast, the EPAS particle cores are enriched in hydrophobic API and the outer surface is enriched in the hydrophilic polymer, with less miscibility than in the SFL powders. Consequently, dissolution rates are faster for the SFL particles, although both techniques enhanced dissolution rates of the API.

Keywords: Particle engineering processes; Precipitation; Freezing

1. Introduction

The influence of active pharmaceutical ingredient (API) solubilization on bioavailability has become increasingly important in the pharmaceutical industry. Many APIs are poorly water soluble with high mucosal permeability [1]. These compounds are classified as biopharmaceutical classification system II compounds for which their maximum bioavailability is limited by their rate of dissolution [2]. Improving the dissolution rate of these compounds is achieved through an increase in surface area available for dissolution by decreasing the particle size of the API and optimizing its wetting characteristics [3] or through complexation with cyclodextrins [4]. Several methods have been used to impose these characteristics on poorly soluble APIs. Milling and solution based techniques have been reviewed extensively [5–7]. Our laboratories have introduced two technologies for enhancing the dissolution rate of a poorly water soluble API by creating nanostructured particles using spray freezing into liquid (SFL) [8–17] and evaporative precipitation into aqueous solution (EPAS) techniques [18–21].

The SFL process creates micronized powders with enhanced dissolution rates. This is a particle engineering

* Corresponding author. College of Pharmacy, University of Texas at Austin, Mailstop A1920, Austin, TX 78712-1074, USA. Tel.: +1 512 471 4681; fax: +1 512 471 7474.
E-mail addresses: kpj@che.utexas.edu (K.P. Johnston), williro@mail.utexas.edu (R.O. Williams).
[1] Co-Corresponding author. Tel.: +1 512 471 4617; fax: +1 512 475 7824.

0939-6411/$ - see front matter © 2005 Elsevier B.V. All rights reserved.
doi:10.1016/j.ejpb.2005.01.002

process that utilizes the atomization of a feed solution containing an API and dissolution enhancing excipient(s) directly into a cryogenic liquid, such as nitrogen. The resulting dried powder is composed of discrete microparticles where the API is molecularly dispersed with a polymer in a porous matrix. This molecular dispersion is achieved by rapid freezing in liquid nitrogen, which prevents phase separation. In previous studies, it was found that enhanced dissolution is due to the amorphous nature of the produced powder, high surface area and enhanced wettability of the SFL nanostructured particles [17]. A schematic representation of the SFL apparatus has been reported [12]. During the SFL process, the API loaded organic solvent is pressurized and atomized via a poly ether–ether ketone (PEEK) nozzle below the surface of liquid nitrogen. Because of the rapid flow rate, liquid–liquid impingement and marked temperature drop in the jet, the emitted solvent is atomized into fine, high surface area microdroplets that are frozen rapidly. The suspension of frozen microdroplets is lyophilized to remove solvent, resulting in an amorphous, micronized powder.

In the EPAS process, the API precipitates due to evaporation of the organic solvent near or above the boiling point and contact with an aqueous solution. A schematic representation of the EPAS process has been reported [21]. The API loaded organic solvent is pressurized, heated and atomized through an elliptical conical stainless steel nozzle into a heated water bath containing stabilizing excipients. The large pressure drop across the small nozzle orifice creates intense atomization with rapid evaporation of the primary organic solvent due to the high temperature of the feed solution and aqueous receiving solution. The rapid evaporation of the feed solvent results in supersaturation, nucleation and precipitation of the API. The excipients within the organic feed solution and/or aqueous receiving vessel stabilize the particles by preventing particle growth and recrystallization of the API precipitates. In addition, the excipients also enhanced the API particle dissolution rate and long term storage stability [21].

The morphology and performance of a nanostructured powder is expected to be highly dependent upon the particle formation process. Solid solution formation can be achieved through co-precipitation or co-melting [3,22]. Co-precipitation and co-melting require supersaturation of the API within the matrix to be limited in time by rapid cooling and rapid removal of solvent so as to inhibit agglomeration of API particles. Solid dispersion formation is achieved through supersaturation and precipitation of the API within the matrix similar to solid solution formation. However, solid dispersions are formed during processes where nucleation and growth of the particles occurs to varying extents or through fusion of the component particles [23].

Because of the nanoscale size of API domains achieved through EPAS and SFL processing, it is difficult to evaluate the particle size and morphology of the powders. Techniques used to evaluate products formed by particle engineering technologies typically include dissolution, X-ray powder diffraction, particle size analysis (laser light scattering or dynamic light scattering), contact angle and surface area analysis. More recently, several authors have utilized atomic force microscopy (AFM) to evaluate nanoparticles adsorbed on to the surface of glass or a film [24–27]. This technique, although useful for assessment of particles, requires that a dispersion be formed and surrounding excipients be removed from the API. This limits the technique for assessment of colloidal dispersions and other dispersible solids. Also, transmission electron microscopy (TEM), in conjunction with staining materials, has been used to evaluate the presence and size of API domains within an excipient matrix [8,28–30]. Z-contrast TEM or STEM dark-field imaging is a novel method for high resolution viewing of API/excipient mixtures without the use of electron density staining or dispersion formation and drying. This tomography process has been used in the semiconductor industry and requires the use of a high-angle annular dark field (HAADF) detector [31]. The high-angle scattering is associated with electron interaction close to the nucleus of the atom. For this reason, the detector is very sensitive to compositional changes and thickness within the specimen. It has not been used previously on pharmaceutical formulations and could prove to be a valuable asset to researchers investigating and characterizing nanoparticles where dispersion in a solvent or staining can remove or mask important morphological features.

The objective of this study was to evaluate and compare particle morphologies produced by the two technologies, SFL and EPAS, in order to assess how morphology impacts the enhancement of the dissolution rate of a poorly water soluble API. The particles were evaluated based on degree of crystallinity, thermal characteristics, dissolution rates and morphologies. The high magnification in Z-contrast STEM provides a clearer view of the morphology at the primary particle level than SEM. STEM micrographs and other particle properties were analyzed in context of the particle formation mechanisms to assess the degree of miscibility of the API and polymer. In the organic SFL solution, both polymer and API nucleate and grow to form amorphous domains during the rapid freezing [10]. In contrast, the presence of an organic–water interface and an aqueous external phase in EPAS provides a driving force during nucleation and growth for the core of the particles to be enriched in hydrophobic API and the outer surface to be enriched in the hydrophilic polymer [21]. Only small amounts of polymer are required at the outer surface to stabilize the particles [19]. API/stabilizer ratios have been as high as 93% for particles with surface areas of 3 m^2/g. It is hypothesized that the differences in the particle formation mechanisms for the EPAS and SFL processes are likely to produce differences in polymer API miscibility and subsequent API bioavailability.

2. Materials and methods

2.1. Materials

Micronized danazol, sodium lauryl sulfate (SLS), polyvinylpyrrolidone (PVP) K-15 and 1.0 N hydrochloric acid (HCl) solution were purchased from Spectrum Chemicals (Gardena, CA). High performance liquid chromatography (HPLC) grade acetonitrile and dichloromethane were obtained from EM Science (Gibbstown, NJ).

2.2. Preparation of SFL micronized powder

A solution of 0.2% w/v danazol and 0.2% w/v PVP K15 was prepared in acetonitrile. Aliquots of the solution were loaded into a high pressure solution cell and atomized beneath the liquid nitrogen surface at 50 ml/min constant flow through a 127 μm ID PEEK nozzle. The PEEK tubing acted as an insulating nozzle that prevented freezing within the nozzle orifice. The constant pressure was supplied by an ISCO syringe pump (Model 100DX; ISCO, Inc., Lincoln, NE). Because of the low viscosity of the acetonitrile API solution, a pressure of only 3000 psi was required to produce a flow rate of 50 ml/min. The frozen microparticles were collected and dried by a VirTis Advantage Tray Lyophilizer (The VirTis Company, Inc., Gardiner, NY). The final powder was protected from moisture and stored under vacuum.

2.3. Preparation of EPAS micronized powder

A solution of 2% w/v danazol and 1% w/v PVP K-15 was prepared in dichloromethane. This solution was pumped via an HPLC pump at 2 ml/min through a heat exchange coil set at 80 °C. After heating, the solution was sprayed under constant pressure of 5000 psi through fine, elliptical, conical nozzle, formed by crimping 0.030 in. ID stainless steel tubing, at ∼5000 psi constant pressure into a heated water bath (80 °C) containing 1% w/v PVP K-15 of equal volume. The resultant dispersion was quenched by injecting it into liquid nitrogen via a syringe and needle and lyophilized to form powder. The final powder was protected from moisture and stored under vacuum.

2.4. Preparation of co-ground physical mixture

A co-ground physical mixture consisting of 3.0 g danazol and 3.0 g PVP was mixed by geometric dilution and ground using a mortar and pestle.

2.5. X-ray powder diffraction (XRD)

A Philips 1710 X-ray diffractometer with a copper target and nickel filter (Philips Electronic Instruments, Inc., Mahwah, NJ) was used to obtain the XRD patterns of the samples. Powder samples were loaded onto aluminum stages having a glass bottom and leveled to a uniform height. The XRD pattern of the leveled powder was measured from 5 to 50 2θ degrees using a step size of 0.05 2θ degrees and a dwell time of 1 s at each step.

2.6. Modulated differential scanning calorimetry (MDSC)

Samples in the range of 10–15 mg of processed and bulk powders were added to crimp sealed aluminum pans and measured on a TA Instruments model 2820 MDSC (New Castle, DE). Samples were heated at a rate of 3 °C/min from 50 to 250 °C at a modulating oscillatory frequency of 1.7 °C/min. Samples were purged with nitrogen gas at 150 ml/min. Glass transition temperatures were measured at the midpoint of the step transition. The MDSC was calibrated using an indium standard.

2.7. Surface area analysis

The specific surface area of the prepared powders was measured using a NOVA-2000 Version 6.11 instrument with NOVA Enhanced Data Reduction Software Version 2.13 (Quantachrome Corporation, Boynton Beach, FL). A known amount of powder (∼200 mg) was loaded into a Quantachrome sample cell and degassed for at least 3 h prior to analysis.

2.8. Contact angle measurement

A 100 mg aliquot of powder was compacted using a Model M Carver Laboratory Press (Fred S. Carver, Inc., Menomonee Falls, WI). The powder pellet was formed with a 500 kg compression force. A 0.03 ml drop of SLS/Tris dissolution media was placed on the compact, and the contact angle between the sample and media was measured using a Model 100–00–115 Goniometer (Ramè-Hart Inc., Mountain Lakes, NJ).

2.9. Scanning electron microscopy (SEM)

A Hitachi S-4500 field emission scanning electron microscope was used to obtain SEM micrographs of the powder samples which had been gold-palladium sputter coated prior to analysis for 45 s. An accelerating voltage of 5 kV was used.

2.10. Environmental scanning electron microscopy (ESEM)

The powder was added to a 1 cm diameter aluminum sample holder and observed using an Enviroscan 2020 (FEI Company, Hillsboro, Oregon) environmental scanning electron microscope with EVEX EDS. The chamber was held constant at 2 Torr with an accelerating voltage of 20 kv.

2.11. Transmission electron microscopy

Samples of the dried powders were placed on 200-mesh carbon-coated copper grids (Electron Microscopy Sciences, Fort Washington, PA) and viewed on a JEOL 2010F transmission electron microscope (JEOL USA, Inc., Peabody, Massachusetts) with a HAADF STEM detector.

2.12. Dissolution

Dissolution testing was performed using a United States Pharmacopeia 27 (USP) apparatus II VanKel VK6010 Dissolution Testing Station with a Vanderkamp VK650A heater/circulator (Varian, Inc., Palo Alto, CA). The inherent low aqueous solubility of danazol required that a solubilizing agent be employed to allow for sufficient wetting and to ensure sink conditions for the powders which were evaluated. Aliquots of 10–15 mg of powder were weighed and placed into 900 ml of SLS/Tris dissolution media. A volume of 5 mL was collected at 2, 5, 10, 20, 30, and 60 min ($n=6$) using a VK8000 autosampler (Varian Inc., Cary, NC). Paddle speed and bath temperature were set at 50 rpm and 37.0 ± 0.2 °C, respectively. A 20 L volume of dissolution media was prepared consisting of 150 g SLS and 242 g Tris that was pH adjusted to 9.0 using 1 N HCl. The collected samples were filtered and evaluated via HPLC at 288 nm using a Shimadzu LC-10 liquid chromatograph (Shimadzu Corporation, Columbia, MD) equipped with an Alltech 5 μm Inertsil ODS-2 C18 reverse-phase column (Alltech Associates, Inc., Deerfield, IL). The danazol peak eluted at 5 min when running mobile phase (70% acetonitrile/30% water, v/v) at 1 ml/min.

3. Results

3.1. Glass transition and contact angles

PVP has been demonstrated to increase the stability of amorphous APIs, by increasing the glass transition temperature (T_g) [32]. Also, PVP has been shown to increase dissolution rates through rapid dispersion upon contact with aqueous media [33]. Table 1 shows the glass transition temperatures of the binary mixtures achieved through each of the technologies studied. The T_g for SFL and EPAS particles were 123.1 and 143.2 °C, respectively. These are lower than both the physical mixture (154.5 °C) and bulk PVP (162.1 °C). MDSC analysis yielded a high, single T_g for the SFL and EPAS particles (Table 1), which is important for stabilization purposes [34]. Due to higher mobility of the amorphous API particles near the glass transition temperature, it is important that the T_g be 50 °C above the highest storage temperature in order to prevent crystallization [35].

Table 1
Glass transition temperatures for the SFL and EPAS samples compared to control and bulk excipients

Sample type	Glass transition temperature (T_g, °C)
SFL danazol/PVP 1/1	123.1
EPAS danazol/PVP 1/1	143.2
Physical mixture	154.5
Bulk PVP	162.1

The Gordon–Taylor equation predicts the glass transition temperature (T_{g12}) for binary mixtures and assumes miscibility and additive free volume of the substrates where w_1 and w_2 are the weight fractions of the individual components and T_{g1} and T_{g2} are their glass transition temperatures:

$$T_{g12} = \frac{w_1 T_{g1} + K w_2 T_{g2}}{w_1 + K w_2}$$

The constant K is defined by Sihma–Boyer rule where T_{g1} and T_{g2} are the glass transition temperatures of the individual components and ρ_1 and ρ_2 are their densities:

$$K \approx \frac{T_{g1}\rho_1}{T_{g2}\rho_2}$$

The T_g for binary mixes of PVP and danazol were calculated as 122 °C using the Gordon–Taylor equation. This predicted value deviated from the measured values of the binary mixes prepared using SFL and EPAS processes. It has been reported that deviation from the Gordon–Taylor equation is through non-uniform distribution of free volumes within the binary mixture [36]. Since the T_g for the mixture processed by SFL (123.1 °C) is near the predicted value, the components are highly miscible in a solid solution. The T_g for the EPAS powder (143.1 °C) is near the midpoint of the T_g of PVP (162.1 °C) and the calculated value for an ideally mixed solution. The significantly larger T_g indicates that a larger fraction of the components is present in a non-uniform distribution of the free volumes. This difference will be shown below to be consistent with the larger primary particle size. The T_g of the physical mixture was 154.5 °C, only 8 °C below that of pure PVP indicating a small amount of miscibility perhaps because of heat increased surface area caused by friction due to mixing using the mortar and pestle. Both EPAS and SFL processed binary mixtures exhibited a greater depression in T_g compared to the physical binary mixtures due to a greater degree of mixing and miscibility.

Similar contact angles were observed for EPAS and SFL powders as shown in (Table 2). The contact angles for aqueous dissolution media on the EPAS and SFL

Table 2
Various characterization results for EPAS and SFL formulations

Characterization technique	EPAS	SFL
BET surface area (m^2/g)	7.41	52.2
Contact angle (°)	26.6	28.0
LLD aggregate particle size (μm)	6.50	3.50

compressed pellets were 26.6 and 28°, respectively, compared to 64.3° for bulk danazol and 37.6° for the physical mixture (data not shown). The low contact angles, or high hydrophilicities suggest significant mixing between the API and stabilizer. For example, if they were completely unmixed in the SFL powder, it is likely the more hydrophobic component, danazol, would favor the surface due to lower surface energy. Instead, a highly hydrophilic surface was present suggesting that the components were mixed with a substantial amount of PVP at the surface, consistent with the T_g measurements. The high wettability of the powders is likely to aid dissolution rates as will be shown below.

3.2. X-ray powder diffraction

The degree of crystallinity in the PVP/danazol mixtures will influence the dissolution rate of the processed powders. The XRD patterns for the bulk danazol, physical mixture control and processed danazol are shown in Fig. 1. The bulk micronized danazol, as received, displayed characteristic 2θ crystalline peaks between 13 and 22.2°. Although with less intense peaks due to dilution, the physical mixture showed a high degree of crystallinity. The XRD pattern for SFL powder lacked crystalline peaks, indicating a completely amorphous morphology as has been seen previously for SFL processed API [10,11,14,17]. The EPAS powder demonstrated a slight peak at the location of the major peak for danazol, indicating a small degree of crystallinity, significantly lower than that of the bulk danazol and physical mixture. In contrast, highly crystalline danazol was produced by EPAS when PVP was used as a stabilizer in the aqueous phase, without using a stabilizer in the organic phase [19]. It is possible that the growing particles crystallized in the aqueous media before enough of the stabilizer (PVP) reached the surface of the particles. Another difference is that the API:surfactant ratio was higher in the previous study which could have prevented the PVP from effectively inhibiting crystallization during particle formation, or after the particles were dried.

The major difference in the present study was that PVP was the only excipient stabilizer, and it was included in both the organic and aqueous phases. As the particles nucleate and grow in the shrinking organic phase droplets during evaporation, the PVP is likely to protect the particle surface more effectively and inhibit crystal growth. Rasenack et al. [37] found that by changing processing conditions or through excipient/stabilizer selection, amorphous API could be formed through precipitation processes.

3.3. Surface morphology

The morphological characteristics of the EPAS and SFL processed powders were examined using ESEM and SEM. Fig. 2a and b show the ESEM micrographs of the powders formed by EPAS and SFL, respectively. The ESEM of the EPAS powder showed a 7–10 μm aggregate composed of many discrete primary nanoparticles that were less than 1 μm in size. The ESEM micrograph of the SFL powder demonstrates a highly porous structure, composed of a nanostructured network of particles. This finding is similar to the SEM micrographs of the SFL powders shown in

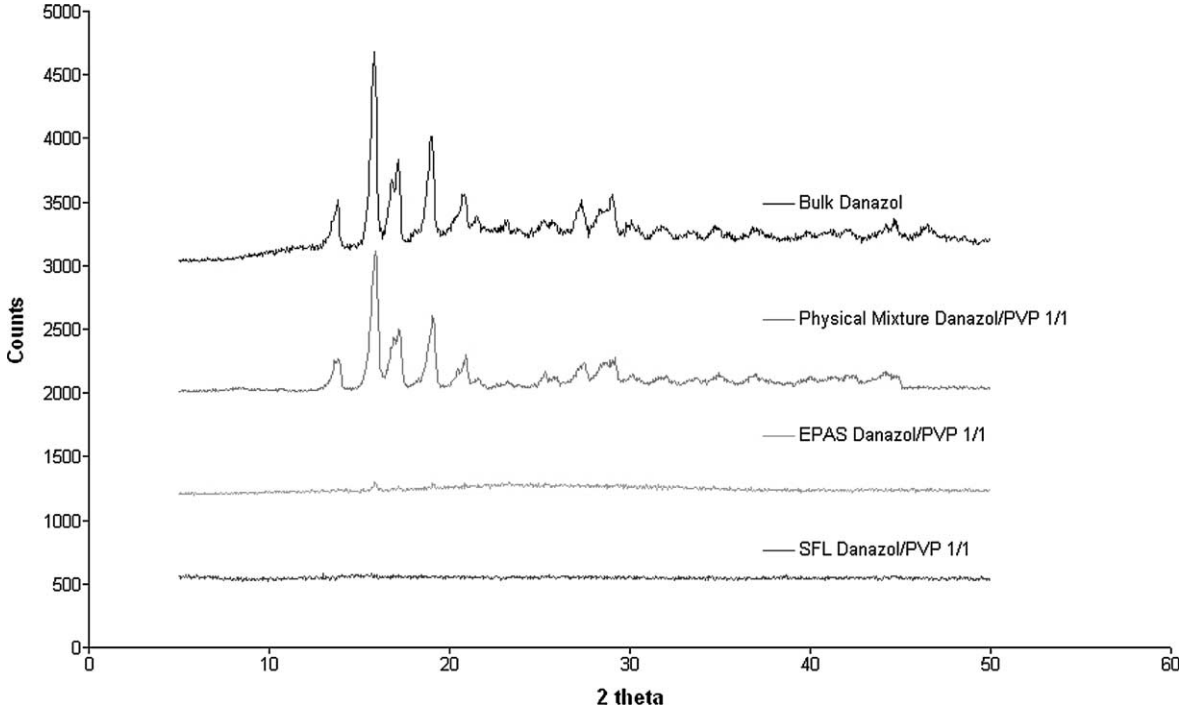

Fig. 1. X-Ray Diffraction patterns for the EPAS and SFL formulations compared to bulk danazol and the physical mixture.

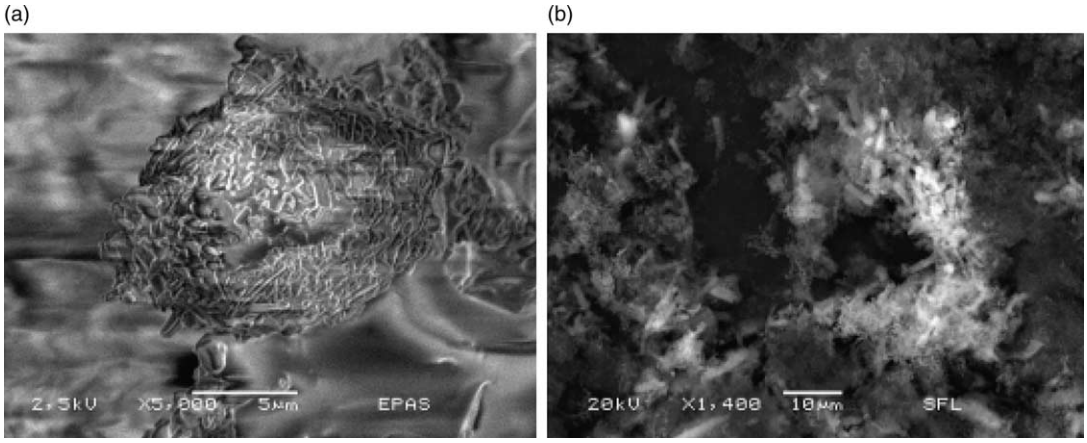

Fig. 2. ESEM micrographs for the EPAS (a) and the SFL (b) powders.

Fig. 3a and b. From the SEM it is evident that the particles formed by the SFL process are highly porous and composed of a nanostructured lattice of polymer and API. The specific surface area shown in Table 2 shows the differences in porosity and primary particle sizes seen in the SFL and EPAS particles, with surface areas of 52.26 and 7.41 m^2/g, respectively.

3.4. Scanning transmission electron microscopy

High resolution Z-contrast STEM was utilized to view the internal morphology of the SFL and EPAS processed powders through mass density analysis. The contrast variation in the STEM is proportional to the mass density of the region multiplied by the atomic number squared (Z) [31]. Regions of high mass density are shown in white. Since the atomic composition and mass density are similar between danazol and PVP, the contrast in the micrographs indicates an overall mass density. These micrographs do not provide direct compositional analysis of the API and polymer mixtures at a given point.

The STEM micrographs of the SFL processed powder are shown in Fig. 4a and b and demonstrate a diffuse grey pattern throughout the particle. Low contrast variation is seen in the mass density throughout the highly interconnected particles, which is indicative of small domain sizes or lack of any large danazol/PVP enriched areas. Bicontinuous curvature is present with regions curved about particles and, in the necks or bridges between particles, regions curved about the pores. It is possible that the bicontinuous curvature indicates spinodal decomposition, although it is very difficult to conclusively delineate the boundary between nucleation and growth and spinodal decomposition [38]. Certainly, the rapid freezing rates have the potential to enter the spinodal decomposition region. The areas of high electron density represent overlapping bridges within the porous SFL particle. The STEM micrograph of the EPAS processed powder is shown in Fig. 4c and d. High contrast variation is evident throughout the EPAS powder due to much larger API/polymer domains. Discrete particles can be seen in the powder through the variations in mass density. These particles are much larger than those produced by SFL. They are not connected by bridges and bicontinuous curvature is not present. The differences in these morphologies are much more apparent in STEM than SEM due to the higher magnification and resolution.

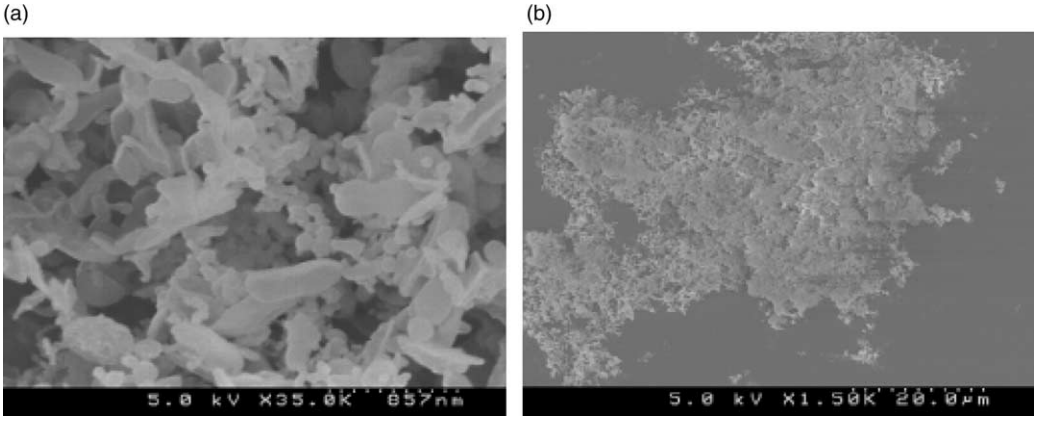

Fig. 3. SEM micrographs of the SFL processed danazol.

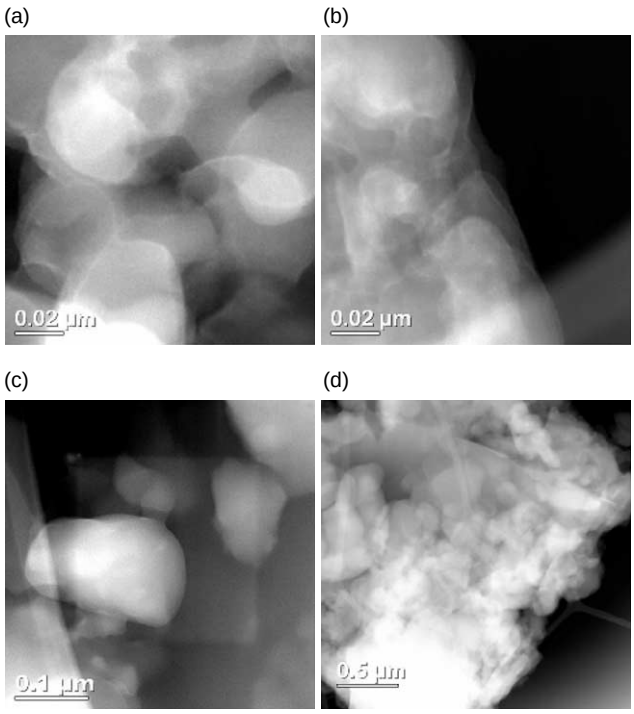

Fig. 4. STEM micrographs of the SFL (a and b) processed danazol and the EPAS (c and d) processed danazol.

3.5. Dissolution

The dissolution profile shown in Fig. 5 illustrates the enhanced dissolution rate achieved through SFL and EPAS processed powders compared to non-processed, bulk danazol. Within the first 2 min, the dissolution of the API was nearly 100% for the SFL powder, compared to 80% for the EPAS processed powder and 40% for bulk danazol, respectively. Within 10 min, the SFL and EPAS dissolution rates were statistically similar, and were statistically much higher than for the bulk danazol.

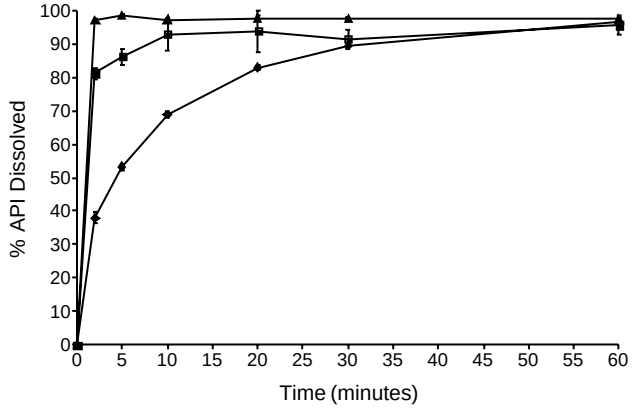

Fig. 5. Dissolution profile for SFL (▲) and EPAS (■) processed danazol compared to the bulk danazol (♦) (USP II, 50 rpm, 0.5% SLS pH 9 Tris buffer, $n=6$).

4. Discussion

The mechanisms of particle formation for the SFL and EPAS technologies differ, and a direct comparison of how these differences affect the particle morphology has not been reported previously. The combination of the MDSC data, the high contrast/high resolution STEM micrographs and an analysis of the phase separation mechanisms in the processes will provide insight into the changes in composition of the particles from the core to the outer surface. The application of the three synergistic methods provides a more detailed description of particle morphology than has been available previously.

The porous morphologies seen in the SEM of SFL particles were composed of nanostructured API-polymer networks on the order of 500 nm in diameter. The high porosity is achieved through the rapid freezing, liquid–liquid impingement and intense atomization. The freezing rate is sufficient such that separation of API and polymer is inhibited and pores are generated by the removal of the solvent during lyophilization. This significantly improves wettability and allows for close proximity of the API to the dissolution media resulting in enhanced wetting and dissolution of API. There are no distinct particle domains indicated on the STEM micrograph. The lack of distinct particles illustrates a dispersion on the molecular level, which is indicative of a solid solution. This is consistent with the hypothesis that the freezing process and nucleation during co-evaporation creates much smaller particle domains than does EPAS processing. This is due to the molecular dispersion of the danazol within the PVP that extends beyond the magnification of the STEM.

EPAS particles, in contrast, were aggregates of larger nanoparticles composed of danazol and PVP according to the ESEM analysis. The smaller number of fine pores reflected the larger primary particles due to particle formation in solution rather than particle formation during freezing. High surface areas were not generated during quench freezing due to the slower freezing rate (quench freezing versus atomization into liquid nitrogen) and higher concentration of API and stabilizer within the frozen material. Since the rate of freezing is slower with quench freezing compared to freezing of atomized droplets, segregation of particles and dissolved solids can occur, yielding lower surface areas [10]. The lack of fine pores indicates that the solvent was not located within these 8–10 μm aggregates since they were formed prior to freeze quenching. The larger primary particle size could be the reason for the smaller surface area and porosity observed in the ESEM micrograph, compared to the SFL particles. These findings were further established through BET specific surface area measurements, where the SFL particles showed significantly higher specific surface area, due to high porosity and a nanostructured network of polymer and API. Through Z-contrast STEM analysis; micrographs of the EPAS processed powders show distinct particles due to

variations in the mass density which caused contrast changes throughout the powder. This further corroborates the results shown in ESEM as well as the establishment of prior particle precipitation and solid dispersion formation.

The SFL process created high surface area, porous, particles composed of submicron primary particles through rapid freezing followed by lyophilization to remove solvent. Betageri et al. [39] reported that the physical traits of a solid solution or solid dispersion formed by lyophilization from a solvent is dependent on the freezing process. Solid solution formation requires that all components be soluble in the solvent during processing [3]. Because of the rapid freezing of a co-dissolved solution of API and stabilizer, the co-precipitation may create a solid solution of amorphous API intermingled with the polymer chain network. The solid solution may be preserved during sublimation of the solvent during lyophilization.

In contrast, the EPAS process creates particles through precipitation in an aqueous solution, where the stabilizer (PVP K-15) is soluble. However, if during EPAS, stabilizer is contained in the organic phase, co-precipitation would be possible as the organic solvent evaporates. Even though the PVP is soluble in water, the chemical potential of PVP in the water appeared to be sufficient to prevent the PVP from leaving the amorphous solid solution in the non-aqueous phase. It appeared that the precipitated particles remain amorphous during the EPAS process due to stabilization by the PVP polymer chains in the amorphous solid solution. Several authors have reported that the inhibitory effect of PVP on crystallization is due to its molecular interaction with the supersaturated API during co-precipitation from a solvent [36,40]. Also, inhibition of crystallization is dependent on API type, API/PVP ratio and the molecular weight and viscosity of the PVP. Previous studies on EPAS have shown that crystallization inhibition does not occur for all APIs when using PVP [21]. The XRD results show that both the SFL and EPAS technologies, when using this API/PVP ratio created amorphous danazol. Also, the single T_g peaks, depressed from that of pure PVP, indicate varying degrees of mixing of danazol within the polymer. Favorable intermolecular interactions between PVP and danazol would aid solid solution formation. Taylor et al. [36] reported that a binary mixture of indomethacin and PVP formed by solvent evaporation created a powder consistent with a glass or a non-equilibrium supercooled liquid due to interactions on the molecular level.

The contributions of each of the previously mentioned attributes of SFL and EPAS powders on dissolution rate were evident in this study. SFL powders had significantly higher dissolution rate compared to both EPAS powders and bulk danazol within the first 2 min of dissolution testing. The higher surface area and greater miscibility of API and PVP in the powders led to the more rapid dissolution of danazol. True solid solutions will dissolve at a rate comparable to the dissolution rate of the stabilizer of a binary mixture under sink conditions [3]. Since PVP is highly soluble in the dissolution media, the dissolution rates of the PVP/API solid solution are enhanced. Since EPAS produced powders have lower porosity, larger primary particle sizes, lower surface area, and less miscibility between the API and PVP, the dissolution rate is slower than that of the SFL powders. However, the surface area is still relatively large and the particles are wetted rapidly leading to significantly faster dissolution than for bulk danazol. Also, after the first 2 min, the rate of dissolution closely resembles that of crystalline bulk danazol. As was indicated through XRD, the EPAS powders were partially crystalline. API that has been rendered amorphous display significantly faster dissolution rate compared to crystalline materials [41]. Taylor and Zografi [36] indicated that the rate of dissolution of binary mixtures of amorphous and crystalline material would show a change in rate following complete dissolution of the amorphous material.

5. Conclusions

Through the use of several characterization techniques, it was shown that the SFL and EPAS technologies form large surface area, wettable powders with rapid dissolution. The STEM revealed 30 nm primary domains in SFL particles and several 100 nm primary domains in EPAS particles, providing unparalleled contrast in mass density across these domains. Based on STEM analysis, measurement of T_g, and the mechanisms of the processes, the SFL process forms powders consistent with a solid solution, whereas EPAS powders tend to be enriched in API towards the center and more enriched in PVP near the surface with a lower degree of miscibility between components. The ability to view contrast in mass density across primary particles on the order of 30 nm offers new insight into particle formation mechanisms that is useful for designing processes and formulations for poorly water soluble APIs with high dissolution rates.

Acknowledgements

The authors wish to gratefully acknowledge financial support from The Dow Chemical Company.

References

[1] J.B. Dressman, C. Reppas, In vitro–in vivo correlations for lipophilic, poorly water-soluble drugs, Eur. J. Pharm. Sci. 11 (2000) S73–S80.
[2] D. Horter, J.B. Dressman, Influence of physicochemical properties on dissolution of drugs in the gastrointestinal tract, Adv. Drug Deliv. Rev. 46 (2001) 75–87.
[3] C. Leuner, J. Dressman, Improving drug solubility for oral delivery using solid dispersions, Eur. J. Pharm. Biopharm. 50 (2000) 47–60.

[4] S.I.F. Badawy, A.L. Marshall, M.M. Ghorab, C.M. Adeyeye, A study of the complexation between danazol and hydrophilic cyclodextrin derivatives, Drug Dev. Ind. Pharm. 22 (1996) 959–966.
[5] T.L. Rogers, K.P. Johnston, R.O. Williams, Solution-based particle formation of pharmaceutical powders by supercritical or compressed fluid CO2 and cryogenic spray-freezing technologies, Drug Dev. Ind. Pharm. 27 (2001) 1003–1015.
[6] E. Reverchon, Supercritical antisolvent precipitation of micro- and nano-particles, J. Supercrit. Fluids 15 (1999) 1–21.
[7] J.H. Hu, K.P. Johnston, R.O. Williams, Nanoparticle engineering processes for enhancing the dissolution rates of poorly water soluble drugs, Drug Dev. Ind. Pharm. 30 (2004) 233–245.
[8] T.L. Rogers, K.A. Overhoff, P. Shah, P. Santiago, M.J. Yacaman, K.P. Johnston, R.O. Williams, Micronized powders of a poorly water soluble drug produced by a spray-freezing into liquid-emulsion process, Eur. J. Pharm. Biopharm. 55 (2003) 161–172.
[9] T.L. Rogers, A.C. Nelsen, M. Sarkari, T.J. Young, K.P. Johnston, R.O. Williams, Enhanced aqueous dissolution of a poorly water soluble drug by novel particle engineering technology: spray-freezing into liquid with atmospheric freeze-drying, Pharm. Res. 20 (2003) 485–493.
[10] T.L. Rogers, A.C. Nelsen, J.H. Hu, J.N. Brown, M. Sarkari, T.J. Young, K.P. Johnston, R.O. Williams, A novel particle engineering technology to enhance dissolution of poorly water soluble drugs: spray-freezing into liquid, Eur. J. Pharm. Biopharm. 54 (2002) 271–280.
[11] T.L. Rogers, K.P. Johnston, R.O. Williams, Physical stability of micronized powders produced by spray-freezing into liquid (SFL) to enhance the dissolution of an insoluble drug, Pharm. Dev. Technol. 8 (2003) 187–197.
[12] T.L. Rogers, J.H. Hu, Z.S. Yu, K.P. Johnston, R.O. Williams, A novel particle engineering technology: spray-freezing into liquid, Int. J. Pharm. 242 (2002) 93–100.
[13] Z.S. Yu, T.L. Rogers, J.H. Hu, K.P. Johnston, R.O. Williams, Preparation and characterization of microparticles containing peptide produced by a novel process: spray freezing into liquid, Eur. J. Pharm. Biopharm. 54 (2002) 221–228.
[14] J.H. Hu, T.L. Rogers, J. Brown, T. Young, K.P. Johnston, R.O. Williams, Improvement of dissolution rates of poorly water soluble APIs using novel spray freezing into liquid technology, Pharm. Res. 19 (2002) 1278–1284.
[15] J.H. Hu, K.P. Johnston, R.O. Williams, Rapid dissolving high potency danazol powders produced by spray freezing into liquid process, Int. J. Pharm. 271 (2004) 145–154.
[16] J.H. Hu, K.P. Johnston, R.O. Williams, Stable amorphous danazol nanostructured powders with rapid dissolution rates produced by spray freezing into liquid, Drug Dev. Ind. Pharm. 30 (2004) 695–704.
[17] J.H. Hu, K.P. Johnston, R.O. Williams, Spray freezing into liquid (SFL) particle engineering technology to enhance dissolution of poorly water soluble drugs: organic solvent versus organic/aqueous co-solvent systems, Eur. J. Pharm. Sci. 20 (2003) 295–303.
[18] X. Chen, Z. Benhayoune, R.O. Williams, K.P. Johnston, Rapid dissolution of high potency itraconazole particles produced by evaporative precipitation into aqueous solution, J. Drug Deliv. Sci. Technol. 14 (2004) 299–304.
[19] X.X. Chen, J.M. Vaughn, M.J. Yacaman, R.O. Williams, K.P. Johnston, Rapid dissolution of high-potency danazol particles produced by evaporative precipitation into aqueous solution, J. Pharm. Sci. 93 (2004) 1867–1878.
[20] X.X. Chen, T.J. Young, M. Sarkari, R.O. Williams, K.P. Johnston, Preparation of cyclosporine A nanoparticles by evaporative precipitation into aqueous solution, Int. J. Pharm. 242 (2002) 3–14.
[21] M. Sarkari, J. Brown, X.X. Chen, S. Swinnea, R.O. Williams, K.P. Johnston, Enhanced drug dissolution using evaporative precipitation into aqueous solution, Int. J. Pharm. 243 (2002) 17–31.
[22] B. Rambali, G. Verreck, L. Baert, D.L. Massart, Itraconazole formulation studies of the melt-extrusion process with mixture design, Drug Dev. Ind. Pharm. 29 (2003) 641–652.
[23] B.M. Tashtoush, Z.S. Al-Qashi, N.M. Najib, In vitro and in vivo evaluation of glibenclamide in solid dispersion systems, Drug Dev. Ind. Pharm. 30 (2004) 601–607.
[24] I. Montasser, H. Fessi, A.W. Coleman, Atomic force microscopy imaging of novel type of polymeric colloidal nanostructures, Eur. J. Pharm. Biopharm. 54 (2002) 281–284.
[25] H. Sato, T. Ohtsu, I. Komasawa, Atomic force microscopy study of ultrafine particles prepared in reverse micelles, J. Colloid Interface Sci. 230 (2000) 200–204.
[26] N. Masaki, K. Machida, H. Kado, K. Yokoyama, T. Tohda, Molecular-resolution images of aspirin crystals with atomic force microscopy, Ultramicroscopy 42 (1992) 1148–1154.
[27] H.Q.G. Shi, L. Farber, J.N. Michaels, A. Dickey, K.C. Thompson, S.D. Shelukar, P.N. Hurter, S.D. Reynolds, M.J. Kaufman, Characterization of crystalline drug nanoparticles using atomic force microscopy and complementary techniques, Pharm. Res. 20 (2003) 479–484.
[28] S.C. Yang, J.B. Zhu, Preparation and characterization of camptothecin solid lipid nanoparticles, Drug Dev. Ind. Pharm. 28 (2002) 265–274.
[29] T. Banerjee, S. Mitra, A.K. Singh, R.K. Sharma, A. Maitra, Preparation, characterization and biodistribution of ultrafine chitosan nanoparticles, Int. J. Pharm. 243 (2002) 93–105.
[30] L.M. Lacava, B.M. Lacava, R.B. Azevedo, Z.G.M. Lacava, N. Buske, A.L. Tronconi, P.C. Morais, Nanoparticle sizing: a comparative study using atomic force microscopy, transmission electron microscopy, and ferromagnetic resonance, J. Magn. Magn. Mater. 225 (2001) 79–83.
[31] P.A. Midgley, M. Weyland, 3D electron microscopy in the physical sciences: the development of Z-contrast and EFTEM tomography, Ultramicroscopy 96 (2003) 413–431.
[32] G. Van den Mooter, M. Wuyts, N. Blaton, R. Busson, P. Grobet, P. Augustijns, R. Kinget, Physical stabilisation of amorphous ketoconazole in solid dispersions with polyvinylpyrrolidone K25, Eur. J. Pharm. Sci. 12 (2001) 261–269.
[33] A.S. Kearney, D.L. Gabriel, S.C. Mehta, G.W. Radebaugh, Effect of polyvinylpyrrolidone on the crystallinity and dissolution rate of solid dispersions of the antiinflammatory Ci-987, Int. J. Pharm. 104 (1994) 169–174.
[34] S. Corveleyn, J.P. Remon, Stability of freeze-dried tablets at different relative humidities, Drug Dev. Ind. Pharm. 25 (1999) 1005–1013.
[35] L. Yu, Amorphous pharmaceutical solids: preparation, characterization and stabilization, Adv. Drug Deliv. Rev. 48 (2001) 27–42.
[36] L.S. Taylor, G. Zografi, Spectroscopic characterization of interactions between PVP and indomethacin in amorphous molecular dispersions, Pharm. Res. 14 (1997) 1691–1698.
[37] N. Rasenack, H. Hartenhauer, B.W. Muller, Microcrystals for dissolution rate enhancement of poorly water-soluble drugs, Int. J. Pharm. 254 (2003) 137–145.
[38] D.J. Dixon, K.P. Johnston, R.A. Bodmeier, Polymeric materials formed by precipitation with a compressed fluid antisolvent, Aiche J. 39 (1993) 127–139.
[39] G.V. Betageri, K.R. Makarla, Enhancement of dissolution of glyburide by solid dispersion and lyophilization techniques, Int. J. Pharm. 126 (1995) 155–160.
[40] M. Yoshioka, B.C. Hancock, G. Zografi, Inhibition of indomethacin crystallization in poly(vinylpyrrolidone) coprecipitates, J. Pharm. Sci. 84 (1995) 983–986.
[41] A.R. Paradkar, B. Chauhan, S. Yamamura, A.P. Pawar, Preparation and characterization of glassy celecoxib, Drug Dev. Ind. Pharm. 29 (2003) 739–744.